International Journal of
Molecular Sciences

MDPI

Article

Poly(A)+ Sensing of Hybridization-Sensitive Fluorescent Oligonucleotide Probe Characterized by Fluorescence Correlation Methods

Bjorn Paulson [1], Yeonhee Shin [2], Akimitsu Okamoto [3], Yeon-Mok Oh [4], Jun Ki Kim [1,2,*] and Chan-Gi Pack [1,2,*]

1 Asan Institute for Life Science, Asan Medical Center, Seoul 05505, Korea; bjorn.paulson+mtrls@gmail.com
2 Department of Convergence Medicine, University of Ulsan College of Medicine, Seoul 05505, Korea; dusgo147@mail.ulsan.ac.kr
3 Research Center for Advanced Science and Technology, The University of Tokyo, 4-6-1 Komaba, Meguro-ku, Tokyo 153-8904, Japan; okamoto@chembio.t.u-tokyo.ac.jp
4 Department of Pulmonary and Critical Care Medicine, University of Ulsan College of Medicine, Seoul 05505, Korea; ymoh55@amc.seoul.kr
* Correspondence: kim@amc.seoul.kr (J.K.K.); changipack@amc.seoul.kr (C.-G.P.); Tel.: +82-2-3010-8619 (J.K.K.); +82-2-3010-8611 (C.-G.P.)

Abstract: Ribonucleic acid (RNA) plays an important role in many cellular processes. Thus, visualizing and quantifying the molecular dynamics of RNA directly in living cells is essential to uncovering their role in RNA metabolism. Among the wide variety of fluorescent probes available for RNA visualization, exciton-controlled hybridization-sensitive fluorescent oligonucleotide (ECHO) probes are useful because of their low fluorescence background. In this study, we apply fluorescence correlation methods to ECHO probes targeting the poly(A) tail of mRNA. In this way, we demonstrate not only the visualization but also the quantification of the interaction between the probe and the target, as well as of the change in the fluorescence brightness and the diffusion coefficient caused by the binding. In particular, the uptake of ECHO probes to detect mRNA is demonstrated in HeLa cells. These results are expected to provide new insights that help us better understand the metabolism of intracellular mRNA.

Keywords: exciton-controlled hybridization-sensitive oligonucleotide probe; fluorescence correlation spectroscopy; dual-color fluorescence cross-correlation spectroscopy; poly(A) tail; mRNA

Citation: Paulson, B.; Shin, Y.; Okamoto, A.; Oh, Y.-M.; Kim, J.K.; Pack, C.-G. Poly(A)+ Sensing of Hybridization-Sensitive Fluorescent Oligonucleotide Probe Characterized by Fluorescence Correlation Methods. *Int. J. Mol. Sci.* **2021**, *22*, 6433. https://doi.org/10.3390/ijms22126433

Academic Editor: Alexandre Mironov

Received: 29 May 2021
Accepted: 14 June 2021
Published: 16 June 2021

1. Introduction

Localizing ribonucleic acids (RNAs) and determining their intracellular dynamics are longstanding challenges in biochemistry and cell biology [1] and are critical for understanding a wide variety of cellular activities [2]. Of particular interest are the synthesis, folding, modification, processing, and degradation of messenger RNA (mRNA), the expression of which is in turn mediated by the dynamics of microRNAs (miRNAs) [3]. While the transport of amino acids is performed by ribosomal RNA (rRNA) [4], numerous non-coding RNAs process rRNA and methylate deoxyribonucleic acid (DNA), synthesize telomeres, and modulate protein function [5]. For example, transfer RNAs (tRNAs) and small nuclear RNAs (snRNAs) catalyze protein synthesis [6] and mRNA splicing [5], respectively. Thus, there is significant interest in applying the high spatial and temporal resolution of optical microscopy to localizing and determining the dynamics of intracellular RNA.

Determining the localization, expression, kinetics, and function of mRNA in live cells has significance for the understanding of gene expression and gene regulation. As mRNAs have no distinguishing features in unstained brightfield microscopy, several techniques have been developed for the in vitro imaging of mRNAs in fluorescent microscopes. Each of these methods has its strengths and drawbacks. The traditional method of fluorescence

in situ hybridization (FISH) requires cells to be fixed and washed to remove nonspecific fluorescence, precluding the visualization of live RNA dynamics. As a result, live-cell fluorescent methods based on oligonucleotides with bound fluorescent labels have been developed. In the commonly used MS2-green fluorescent protein (GFP) system, mRNA is tagged via the genetic incorporation of RNA stem loops that bind the fluorescent proteins [1,7,8]. Numerous derivative probes and improvements to the original MS2-GFP system have been proposed, including reporters with shorter and more configurable RNA binding domains [9,10], repeating strings of fluorescent proteins for increased brightness [10], and split protein complexes that fluoresce conditionally in the case of correct RNA hybridization [11]. FISH has also been recently adapted via endogenous probes for use on live cells [12,13]. However, all these methods require the insertion of reporter genes into the target cell or organism.

As an alternative, the treatment of cells with exogenous RNA-targeting probes can be used to reveal RNA dynamics, as has been demonstrated by the injection of labeled mRNA into oligodendrocytes [14]. Similar probes for tracking RNA in living cells include functionalized quantum dots, which provide high photostability and brightness [7,15,16]; nucleic acid stains [7,17]; probes based on colloidal gold [7,18] and silica [19] nanoparticles; and synthesized DNA-based probes, such as molecular beacons [20,21]. The common methods for the transfection of these probes include microinjection [20], electroporation, and reagent-based methods.

However, many of these probes have low fluorescence specificity for RNA sequences, resulting in a high fluorescence background, and often, several probes are required to bind to a single RNA molecule and obtain consistently observable fluorescence. More recently-developed fluorescent probes for RNA visualization solve the problem of background fluorescence by using RNA hybridization-specific fluorescence. Exciton-controlled hybridization-sensitive oligonucleotide (ECHO) probes exploit the self-quenching, non-covalent dimers of fluorescent dyes that dissociate during hybridization to allow strong RNA-tagged/targeted fluorescence and re-form quenching dimers upon dehybridization to achieve a low fluorescence background [1,22]. These "turn-on probes" have been further enhanced using locked nucleic acids (LNA) for increased stability and single nucleotide polymorphism (SNP)-targetable fluorescence [23]. They have also taken inspiration from miRNA, hybridizing to the poly(A) tail of mRNA [22,24,25].

In almost all eukaryotic cells, complete mRNA are stabilized and prepared for intracellular transport by polyadenylation, which includes the addition of a poly(A) tail to the 3′ end of the RNA molecule. In addition to providing protection against degradation, polyadenylation enables mRNA diffusion/transport from the nucleus via ribosomes for protein synthesis. Transient polyadenylation has also been associated with targeted degradation of cytoplasmic RNA [26], indicating that the intracellular expression of poly(A) is worthy of further scrutiny.

Most of the previous studies applying DNA-based probes, such as the ECHO probe, have focused on single-particle visualization and localization of intracellular mRNA, and there have been few quantitative studies on the dynamic properties of mRNA. While single-molecule detection using GFP or cyanine dye probes has been applied to observe the processes underlying the mRNA metabolism, including the modulation of mRNA decay by promoter proteins [27], it may be of interest to introduce a small-molecule system into cells that allows for the quantification of mRNA dynamics, such as ECHO. As it is still unclear how mRNAs spread throughout individual cells, knowledge of probe dynamics would facilitate quantitative determination of the intracellular kinetic properties of the target mRNA.

Fluorescence correlation spectroscopy (FCS) and dual-color fluorescence cross-correlation spectroscopy (FCCS) are highly sensitive methods for determining the molecular diffusion dynamics and interactions of probe-bound moieties in both aqueous solution and live cells. Based on random fluctuations in fluorescence from a small detection volume as fluorophores are quenched, relaxed, or emitted or transit the volume in question, a correlation

function experimentally obtained by FCS can be fit based on kinematic models to determine the state transition parameters or diffusion coefficients (see also Section 4. Materials and Methods). In comparison with other conventional methods, FCS is also robust against absolute concentration and fluidic viscosity, which both. have high local variance in living cells [28,29]. FCS is particularly useful for tracking the diffusional motion of nanoparticles taken up into cells by endocytosis [19,30–34]. Shin et al. have previously used FCS methods to characterize the dark-state and triplet relaxation time of ECHO probes in terms of a two-state excitation model [35]. However, the probes' luminescence, diffusion coefficients, and kinetic properties have not been previously determined in the cellular environment. Of particular interest are their intracellular behaviors and multi-channel fluorescence capabilities. Furthermore, multi-fluorophore fluorescence, which enables dual-color FCCS, can be useful because it enables enhanced sequence specificity (i.e., molecular interaction) and higher fluorescence signals. Thus, FCCS is promising for detecting the molecular dynamics and kinetics of RNA-bound fluorescence probes in live cells and aqueous solutions.

In this study, thiazole-orange-based ECHO fluorescence probes with different excitation wavelength (D_{nnn}) designs were combined with FCS and FCCS analyses to achieve insight into the changes in the probes' fluorescence and diffusion dynamics, both in medium and within cells [22]. The fluorescence intensity of all five D_{nnn} probes was shown to increase markedly with poly(A) hybridization, with the increases ranging from 1.5× to 12× and with the highest hybridization fluorescence gain occurring for D_{514}. Based on the FCS analyses in solution, the diffusion was characterized by a two-component diffusion model, with fast diffusion coefficients around 120 $\mu m^2/s$ corresponding to free D_{nnn} probes and slow coefficients around 9 $\mu m^2/s$ corresponding to D_{nnn} complexes with a target. The dual-colored fluorescence was quantified by FCCS using a one- or two-component diffusion model. An increasing brightness and a dependence on poly(A) concentration were revealed as mixes of two different D_{nnn} probes bound to poly(A). Based on the evidence of poly(A) binding, it can be concluded that the probes were transiently transfected into cells by electroporation and by using a reagent. The strong fluorescence intensities persisted in the cells, allowing for intracellular comparison of diffusion and transfection behaviors between poly(A) tails under different transfection methods. The measured diffusion coefficients were in good agreement with the results of previous studies on intracellular diffusion and contrasted sharply with those using a transfected non-interfering GFP. Overall, the results indicate that the application of the ECHO probe to an analysis of intracellular mRNA dynamics and metabolism is a promising approach when combined with fluorescence correlation methods.

2. Results

A series of hybridizing ECHO probes D_{nnn} were synthesized by a conventional phosphoramidite method [36]. When in the non-hybridized state, these probes undergo fluorescence quenching due to excitonic interactions. As described in detail in a previous paper [22], each fluorescence probe was designed for fluorescence excitation at a specific wavelength *nnn* (in nm). These probes become significantly more fluorescent when hybridizing into DNA and RNA, as the intercalation of the dye into the nucleic acid structure separates the dimers and deactivates quenching via non-emissive transitions [37]. For this study, D_{nnn} fluorophores were incorporated into poly(T) chains, as shown in Figure 1a, to enable hybridization to targets, such as the poly(A) sequence and poly(A) tail of mRNA. The 5′-d($T_6D_{nnn}T_6$)-3′ poly(T) chain is long enough to be specific for poly(A) while also being short enough to allow multiple particles to hybridize to individual poly(A) targets. In human cells, mRNA poly(A) tails tend to be between 250 and 300 adenines in length [38], allowing for the hybridization of multiple fluorescent probes to the same tail. The schematics of the probe, the schematic hybridization of a single-color fluorescent probe, and simultaneous multi-color ECHO hybridization are illustrated in Figure 1a–c, respectively. When transfected using a reagent or electroporated into the HeLa cells, the 5′-d($T_6D_{nnn}T_6$)-3′-tagged mRNA fluoresces from the nucleus and cytosol, allowing for

the detection and tracking of mRNA dynamics by confocal microscopy and fluorescence correlation methods (Figure 1d,e).

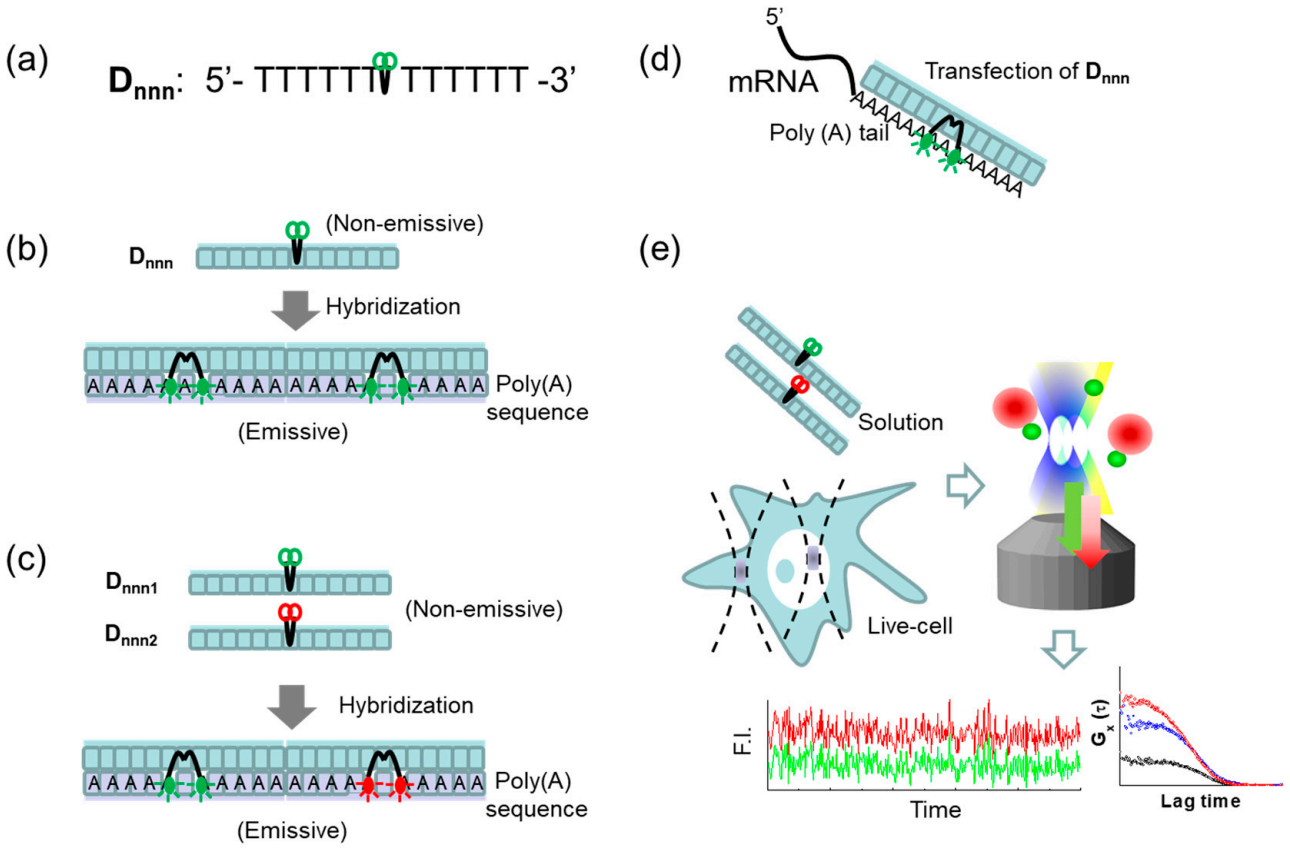

Figure 1. Schematic diagram of hybridization-sensitive fluorescent DNA (D_{nnn}) probes selectively sensing a poly(A) sequence and the detection of D_{nnn} by fluorescence correlation methods. (**a**) The structure of the D_{nnn} probe molecules, consisting of 12 thymine sequences and 2 organic dye molecules (green). The subscript *nnn* denotes the excitation wavelength in nm. (**b**) Schematic representation of a single-color D_{nnn} probe, detected by FCS, before and after hybridization with the target poly(A) sequence. (**c**) Schematic representation of dual-color D_{nnn} probes monitored by dual-color FCCS before and after simultaneous hybridization with the target sequence. (**d**) Schematic representation of D_{nnn} probe hybridized with poly(A) tail of mRNAs in live cell after reagent transfection or electroporation to live cells. (**e**) Schematic representation of FCS and FCCS measurements of sample in aqueous solution and in a live cell after transfection of D_{nnn} probe. F.I. stands for averaged fluorescence intensity, presented in counts per second (CPS; or kHz). $G_x(\tau)$ denotes the two fluorescence auto-correlation functions (blue and red) and the cross-correlation function (black; see also Section 4. Materials and Methods).

Fluorescence Behavior of D_{nnn} before and after Hybridization with Poly(A) Oligomer

Although the fluorescence deactivation of the D_{nnn} probes via dehybridiziation has previously been demonstrated, and their absorption and fluorescence spectra in water are well known [37], their diffusion characteristics and hydrodynamic properties before and after hybridization have not been previously measured in aqueous solution. Figure 2a–e show the FCS evaluations of DNA probes at five different wavelengths before and after hybridization with poly(A) oligomer. All the probes demonstrated significant increases in average fluorescence intensity (CPS) after hybridization (Figure 2f), which is in good agreement with the result of a previous study [36]. While fluorescence intensity was not sufficient to confidently fit non-hybridized D_{nnn} probe diffusion, except for that of D_{436}, the fluorescence correlation functions $G(\tau)$ after hybridization were fit to a two-component model, as described in the Methods section, where the first ("fast") component captured the effective diffusion coefficient of the free probe molecule in the medium, and the second ("slow") component captured the effective diffusion due to interactions

with poly(A) oligomer. The fast diffusion component was approximately 120 μm^2/s, corresponding to the values predicted from the molecular weight of the probe (~5 kD), while the slow diffusion components were 10.5, 6.8, 9.5, 9.2 and 9.8 μm^2/s for the D_{nnn} complex, including poly(A) oligomer with *nnn* = 436, 488, 514, 600 and 640 nm, respectively. The diffusion coefficients of the complexes formed by each probe were approximately 12 times smaller than that of the free diffusion probe, which corresponds to the diffusion coefficient of linear double-stranded DNA with a size of approximately 300 bp [39,40]. The averaged fluorescence intensity ratios between D_{nnn} after and before hybridization ranged from 1.52 for D_{436} to 11.37 for D_{514}. Although it is unclear why the rate of change of fluorescence intensity varied depending on the type of probe, this may have been caused by the instability of the electrochemical properties of the dye used or the intercalation of the dye to DNA.

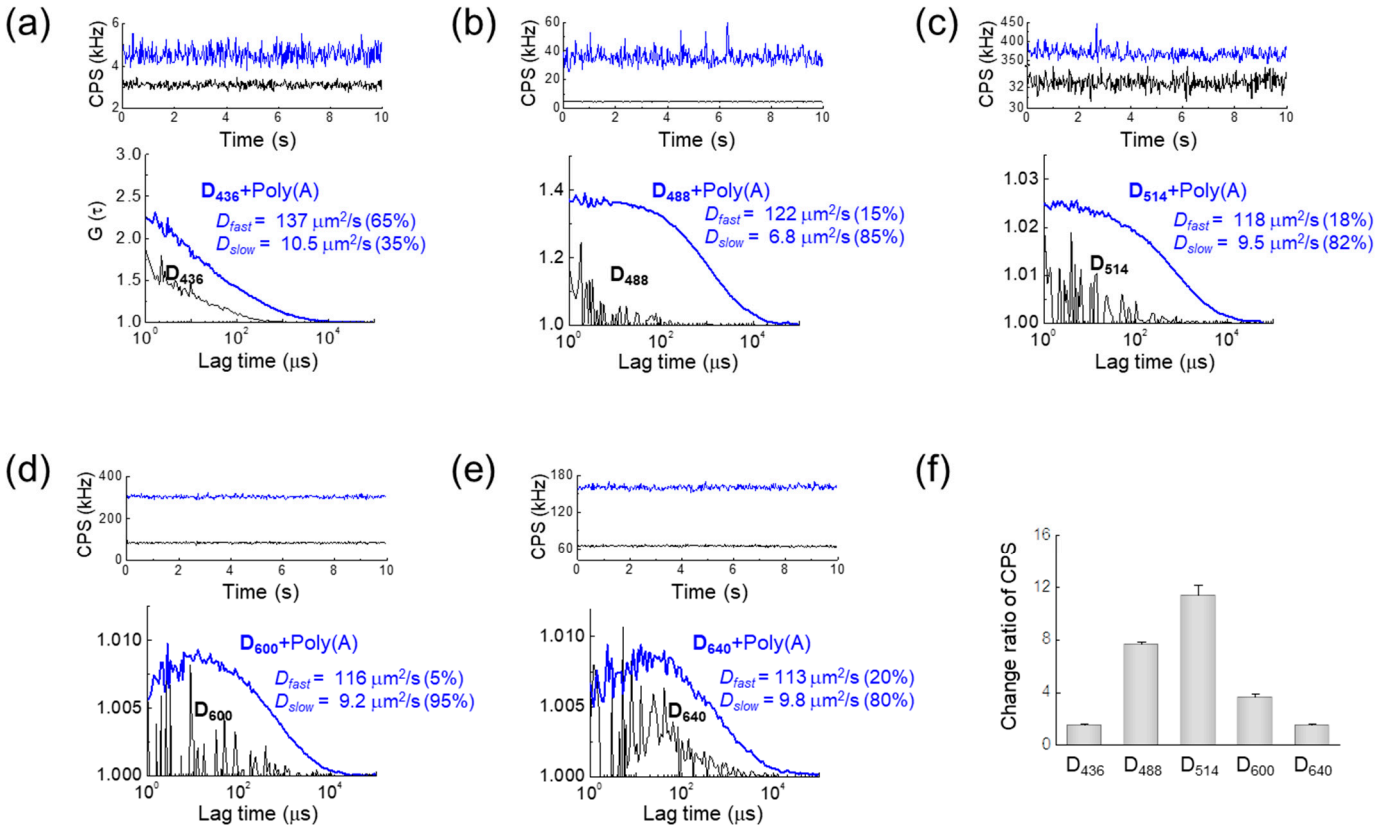

Figure 2. Detection of DNA probe hybridization with poly(A) oligomers by fluorescence correlation spectroscopy for the (**a**) D_{436}, (**b**) D_{488}, (**c**) D_{514}, (**d**) D_{600}, and (**e**) D_{640} probes. The subscripts indicate the principal excitation wavelength (nm). (top) Representative averaged fluorescence intensity traces (CPS; kHz) for D_{nnn} probes alone (black) and hybridized to poly(A) oligomer (blue). (bottom) Fluorescence correlation function $G(\tau)$ between the different dyes before (black) and after (blue) hybridization. The mean diffusion coefficients (D_{fast} and D_{slow}) of the free D_{nnn} probe and hybridized D_{nnn} complex with poly(A) oligomer are also shown (inset). (**f**) Ratio of averaged fluorescence intensity after and before hybridization for each D_{nnn} probe.

Following the FCS on single-color D_{nnn} + poly(A) compounds, dual-color D_{nnn} mixtures were prepared with D_{488} and D_{640} at a 1.75:1 molar ratio and co-hybridized with sample poly(A) oligonucleotides. As shown in Figure 3, increasing the poly(A) concentration from 4.56 to 45.6 μM greatly decreased the relative fluorescence of D_{640} over D_{488}. The fluorescence intensity (CPS) ratio of D_{488} to D_{640} was 0.043:1 at 4.56 μM, whereas it was 0.73:1 with 45.6 μM poly(A). As a result, the relative cross-correlation amplitude (RCA) decreased from 0.92 to 0.35 as the poly(A) concentration was increased, indicating that the number of probes was insufficient due to an increase in the excess poly(A) oligomer. This

result demonstrates that using a dual-color probe combined with FCCS makes it possible to detect the binding specifically with the target, which includes gathering information on the binding between the probes as well as on the diffusion coefficient.

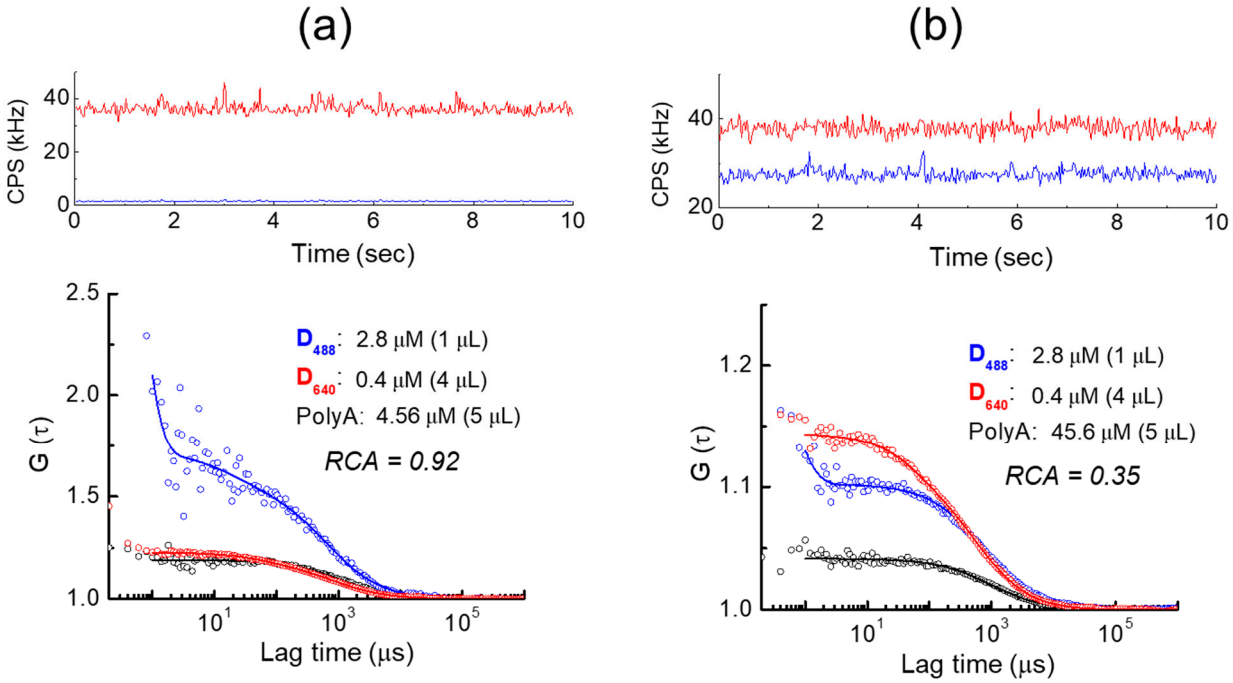

Figure 3. Detection by FCCS of the simultaneous hybridization of two different D_{nnn} probes with poly(A) oligomers. (**a**) Representative fluorescence intensity traces (top) for a mixture of D_{488} and D_{640} probes with 4.56-μM poly(A), resulting in three fluorescence correlation functions (bottom) and a relative cross-correlation amplitude (RCA) of 0.92. (**b**) Representative fluorescence intensity traces (top) for the same mixture with 45.6-μM poly(A), resulting in fluorescence correlation functions (bottom) with similar diffusion coefficients but an RCA of 0.35. The fluorescence auto-correlation functions of D_{488} and D_{640} are represented in blue and red, respectively. The fluorescence cross-correlation function of the two probes is represented in black.

In Figure 4, the results of the transient transfection and electroporation of 5′-d($T_6D_{514}T_6$)-3′ into HeLa cells are shown and compared with the electroporation of GFP. A high probe concentration (strong fluorescence) is required for cell imaging using a confocal microscope, whereas FCS analysis is characterized by a high sensitivity at a low concentration (less than 1 μM). Thus, a relatively small concentration of probes was used here compared with that used in most previous studies. As can be seen, 12 h after the electroporation of D_{514} probe into the HeLa cell, the fluorescent probes accumulated into a relatively small number of puncta in the cytoplasm surrounding the nucleus, indicating the agglomeration of probe-tagged mRNA. In contrast, after 3 h of transfection of the D_{514} probe, the fluorescence was widely spread across many smaller fluorescent puncta in the cytoplasm, indicating a relatively uniform uptake throughout the cytoplasm without agglomeration, although any apparent localization may also be partially due to localized enzymatic degradation of the nucleic acid probe [41]. Interestingly, although it should be expected that electroporation will transfer the probe to the cell nucleus, both the electroporation and transfection methods showed that the probe was concentrated more in the cytoplasm than the cell nucleus. Despite their distinct appearances, the diffusion rates of the electroporated and transfected samples were similar, with mean diffusion coefficients between 0.78 and 0.80 $\mu m^2/s$ in the cell, respectively (Table 1). In the culture medium, they exhibited similar mean diffusion coefficients of 41.2 and 46.5 $\mu m^2/s$, respectively. These values are 2.5 times lower than the diffusion coefficients of the probe obtained in distilled water, indicating that D_{514} was hybridized to an unknown DNA fragment with the poly(A) sequence contained in the

culture medium. In both cases, the electroporated GFP was an order of magnitude more diffusive, with intracellular diffusion coefficients of 21 $\mu m^2/s$ in cell and 74 $\mu m^2/s$ in culture medium, reflecting the increased viscosity in the cell [42]. The diffusion of D_{514} samples in HeLa cells fit a two-component model, despite the same samples in culture medium fitting a one-component model. In contrast, the diffusion of GFP in both HeLa cells and media solution fit a one-component model [42].

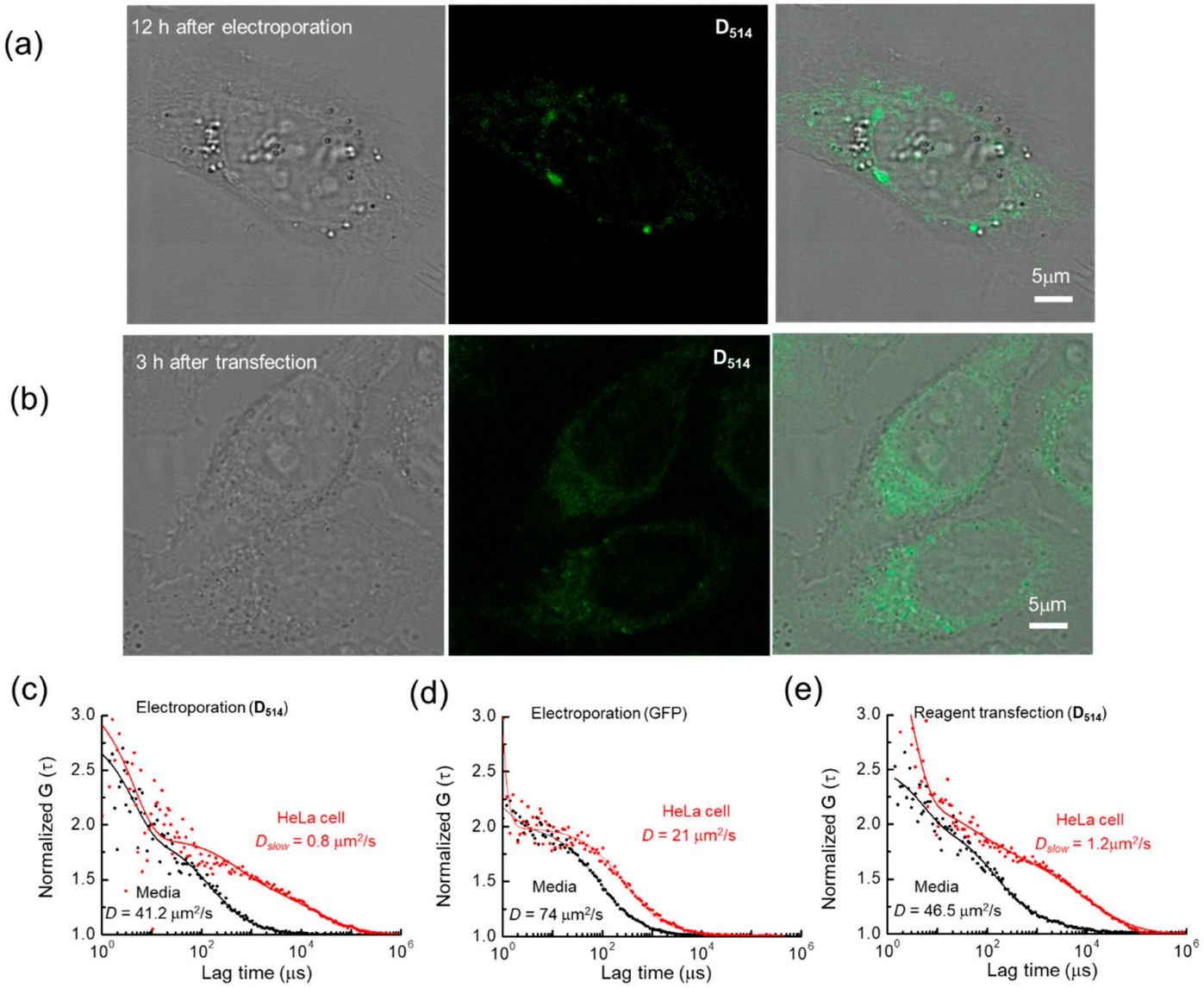

Figure 4. FCS analysis of live HeLa cells transfected with the D_{514} probe. (**a**) HeLa cell after 12 h of electroporation with the D_{514} probe (scale bar: 5 μm). (**b**) HeLa cell after 3 h of transfection with the D_{514} probe (scale bar: 5 μm). (**c**) Representative fluorescence auto-correlation function of the D_{514} probe and (**d**) recombinant GFP molecule in live HeLa cells after electroporation. (**e**) Representative fluorescence auto-correlation functions of the D_{514} probe in live HeLa cells after 3 h of transfection. The black and red curves (solid) are functions fit to the spectra from the culture medium and live cells, respectively. The D value of the D_{514} probe obtained from the fitted curve is also shown (inset). For simplicity, only the diffusion coefficient of the slow component is shown to represent the mobility in the live cells.

Table 1. Comparison of mean diffusion coefficients D of the D_{514} probe and GFP in medium and in HeLa cells.

Fluorescent Probe	D ($\mu m^2/s$)	
	Medium	**HeLa**
GFP (Electroporation)	74	21
5′-d(T6D_{514}T6)-3′ (Electroporation)	41.20	0.78
5′-d(T6D_{514}T6)-3′ (Reagent transfection)	46.50	0.80

As shown in Figure 5, a range of diffusion coefficient D values (D_{slow}) were measured for the D_{514} probe in HeLa cells. The minimum, median, and maximum values of the measured diffusion coefficients were 0.05, 0.57, and 3.3, respectively, in the case of electroporation and 0.04, 0.63 and 3.3, respectively, in the case of reagent transfection. This result demonstrates that the diffusion coefficient of D_{nnn} introduced into the cell did not differ significantly between the two methods. Importantly, these small diffusion coefficient values correspond to several kbps, considering the high viscosity (increased by approximately 3.5 times) in the cell [42].

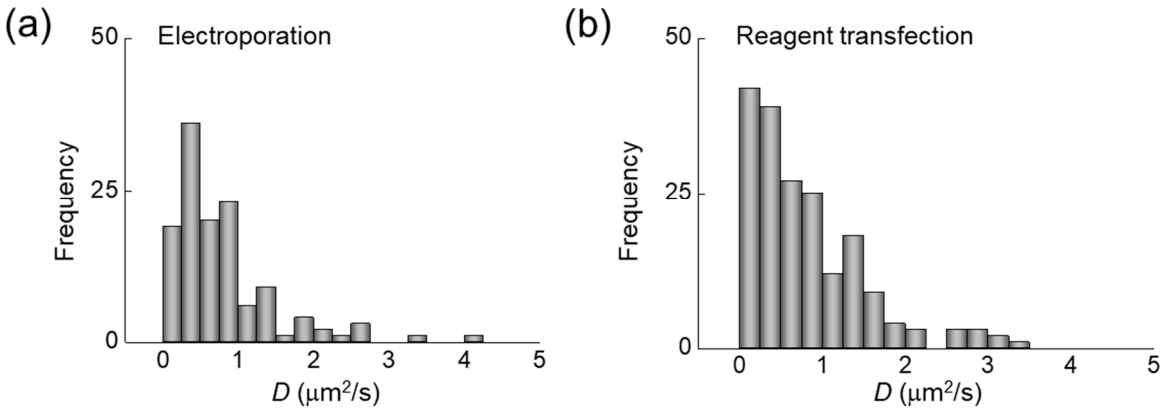

Figure 5. Summary of measured diffusion coefficient D values of the D_{514} probe in live HeLa cells (n = 15). The histograms show D values for the D_{514} probe in HeLa cells after (**a**) electroporation and (**b**) transient transfection using a reagent. For simplicity, only the diffusion coefficient of the slow component is shown.

3. Discussion

It was expected that the precise localization of the synthesized DNA-based fluorescent ECHO probe would be assisted by its low background fluorescence and high fluorescence upon hybridization. Due to the exciton-based quenching between fluorophores, the D_{nnn} probes exhibited very little fluorescence prior to hybridization. In this study, the fluorescence intensity was enhanced by a factor of between 1.25 and 11.37 upon mixing with a solution of poly(A) ribonucleotide chains. This fluorescence enhancement agrees with the results of prior studies on the binding of ECHO probes to RNA [22,23]. It is also comparable to those of certain probes based on molecular beacon technology, although some molecular beacons have exhibited an order of magnitude more specificity to hybridization [43–45]. Expanding on previous studies [35] that determined the band structure of D_{nnn} and measured its relative diffusion in various buffers and viscosities, the present study aims to establish the diffusion characteristics of D_{nnn} probes in water and live cells and definitively determine whether mRNA binding is occurring.

The fluorescence correlation function characteristics of poly(A) oligomer were successfully detected from both the single- and double-colored DNA-based D_{nnn} probes. On

the single-colored DNA probe in aqueous solution (i.e., distilled water), FCS generated fluorescence correlation functions that fit well with the two-component diffusion model. The fast diffusion component D_{fast} represents the diffusion of the free probes in aqueous solution, and its value varied between 113 and 137 $\mu m^2/s$. In contrast, the slow diffusion component D_{slow} represents the slow diffusion of the hybridized D_{nnn}-poly(A) complexes in aqueous solution, and its value varied between 6.8 and 10.5 $\mu m^2/s$. Using single-particle tracking, Tadakuma et al. reported a diffusion coefficient of approximately 30 $\mu m^2/s$ for mRNA tagged with exogenous enhanced GFP (EGFP) in water along with a diffusion coefficient of 0.2 $\mu m^2/s$ for intron-free EGFP-mRNA in the nucleus [46].

Following the FCS evaluation on single-color D_{nnn} in aqueous solution, dual-color D_{nnn} mixtures were prepared for FCCS analysis with D_{488} and D_{640} co-hybridized with sample poly(A) oligonucleotides. The RCA between the dual probe channels was observed to decrease from 0.92 to 0.35 as poly(A) oligomer concentration was increased. Although this indicates strong binding to mRNA molecules, these molecules are frequently bound only to a single fluorophore at high poly(A) concentrations. Examinations thus revealed a low cross-correlation between different fluorophores. In contrast, when the poly(A) concentration is low, the binding capacity of the poly(A) saturates, resulting in a great number of poly(A) moieties being host to a mix of probes, which, in turn, have highly correlated fluorescence.

The strong sensitivity of fluorescence to hybridization simplified the assessment of cellular uptake. The uptake by electroporation and reagent transfection was assessed in HeLa cells with the D_{514} probe. When transfected or electroporated into the HeLa cell, the D_{nnn}-tagged mRNA detected by confocal microscopy was localized to the perinuclear region and the cytosol, allowing the detection and tracking of mRNA dynamics. The electroporated cells expressed punctate fluorescence, with large agglomerations in clumps in the perinuclear region, while the transfected cells expressed fluorescence diffused throughout the cytoplasm. The variance in the patterns of expression was surprising, as the probe was expected to target the poly(A) tails of mRNA, which should be the same in both cases. Although the current images are slightly unclear, electroporated mRNA probes appeared to be highly localized to the cytoplasm. Further examination should be given to determining the cause of this localization, particularly as to whether it arises due to the characteristics of the probe or due to the sensitivity of the intracellular environment to the internalization method. One potential factor in the apparent probe localization is the digestion of the D_{nnn} probes or hybridized RNA due to localized enzymatic degradation. The intracellular degradation of $T6D_{535}T6$ has previously been determined to result in a 50% reduction in fluorescence over 6 hours [41]. While degradation of the probes or bound RNA may quench fluorescence, affecting the apparent probe localization, probe degradation is not rapid enough to cause measurable error in FCS measurements. In contrast, the cleaving of RNA adjacent to the probe hybridization site could contribute to the measured fast diffusion fraction, but an increase in the fast diffusion fraction is not observed. The measured diffusion coefficients of 0.8 and 1.2 $\mu m^2/s$ were slightly higher than those previously documented for the Brownian motion of β-globin and EGFP mRNAs directly injected into the nucleus [46].

The strong fluorescence enhancement upon hybridization with the target sequence and the uptake of the D_{514} probe into the cell offers the opportunity to compare the diffusion rates in the culture medium with those in the cell. The probes in the electroporated HeLa cells exhibited a slow diffusion rate 50 times lower than in medium, while those in the transfected HeLa cells exhibited a diffusion rate 40 times lower. In contrast, when electroporated into HeLa cells alone, the non-hybridizing GFP exhibited a diffusion rate 3.5 times lower than in medium. This provides strong evidence that the diffusion of the probes in the cytosol was not primarily mediated by viscosity and hydrodynamic diameter, as in the case of GFP, but that a significant amount of binding, localization, and perhaps even functional activity of the attached mRNA significantly slowed D_{514} diffusion in the cell. The measured diffusion coefficients were characteristic of mRNA diffusion in cells and

were slightly higher than the previously measured diffusion coefficient of 0.2 $\mu m^2/s$ for intron-free EGFP-mRNA in the nucleus [46]. The slight discrepancy with this prior study may be due to the size and hydrodynamic diameter of the bound mRNA.

Diffusion methods have previously been used to demonstrate the stability and immobility of D_{514} probes for ECHO-live FISH imaging in HeLa cells. A D_{514}-$(U)_{22}$ probe was observed to result in a diffusion coefficient of 0.0004 ± 0.0021 $\mu m^2/s$ [13], while D_{514} probes bonded to large nanoparticles have exhibited restricted diffusion across the nuclear membrane [47]. Thus, as a proof-of-concept, this study demonstrates the first measurement of the free diffusion coefficient of the D_{514} probe in the cellular environment.

Taken together, the combination of fluorescence enhancement, dual-color fluorescence, D values, and intracellular dynamics indicate that the D_{nnn} probes bound strongly to mRNA and tracked their dynamics throughout the cell. While this study demonstrates a proof-of-concept, dual-color method for FCCS via the hybridized fluorescent tagging of RNA, the establishment of these methods is expected to facilitate the visualization and understanding of the function and metabolism of intracellular mRNAs. Further application of these nucleic acid-based probes will be required to discover the ties between the observed dynamics and the full behavior of mRNA in the cellular microenvironment(s).

4. Materials and Methods

4.1. Cell Culture

A human cancer cell line (HeLa) was obtained from the Korea Cell Line Bank and grown in Dulbecco's modified Eagle's medium (DMEM) and fetal bovine serum (FBS; Gibco, ThermoFischer Scientific Korea Ltd., Seoul, Korea). Culturing reagents were purchased from Sigma-Aldrich, St. Louis, MO, USA. Cells were cultured at 37 °C in DMEM containing 10% FBS, 100-U/mL penicillin, and 100-U/mL streptomycin under a humidified 5% CO_2 atmosphere.

4.2. Confocal Laser Scanning Microscopy

Fluorescence confocal microscopy was performed on a LSM510 confocal microscope (Carl Zeiss, Jena, Germany). Illuminations were provided by Ar^+ ions for a wavelength of 514 nm via a 40× water-immersion objective lens (C-Apochromat, 40×, 1.2 NA; Carl Zeiss). The pinhole size was adjusted to 70 μm.

4.3. Fluorescence Correlation Spectroscopy and Fluorescence Cross-Correlation Spectroscopy

The fluorescence correlation analysis has been described in detail in previous papers [35]. Briefly, FCS and FCCS measurements were carried out using a ConfoCor 2 (Carl Zeiss) built on an LSM510 confocal microscope (Carl Zeiss) via a 40× water-immersion objective lens (C-Apochromat, 40×, 1.2 NA; Carl Zeiss). Illuminations were provided by Ar^+ ions for wavelengths of 458, 488, and 514 nm, and an He–Ne laser for wavelengths of 543 and 633 nm via a 40× water-immersion objective lens (C-Apochromat, 40×, 1.2 NA; Carl Zeiss). Fluorescence was collected using an avalanche photodiode (SPCM-200-PQ; EG&G). Appropriate excitation laser and fluorescent filters were used for each color probe (D_{436}: Ex 458 nm, Em 475 nm long-pass filter (LP); D_{488}: Ex 488 nm, Em 505 nm LP; D_{514}: Ex 514, Em 530−600 nm; D_{600}: Ex 543 nm, Em 560 nm LP; D_{640}: Ex 633 nm, Em 650 nm LP). The fluorescence correlation functions $G_x(\tau)$ were calculated using the following equation:

$$G_x(\tau) = 1 + \frac{\langle \delta I_i(t) \cdot \delta I_j(t+\tau) \rangle}{\langle I_i(t) \rangle \langle I_j(t) \rangle}, \quad (1)$$

where τ denotes the time delay; I_i denotes the fluorescence intensity of channel i (r = red, g = green); and $G_r(\tau)$, $G_g(\tau)$, and $G_c(\tau)$ denote the auto-correlation function of the red channel ($i = j = x = r$), the auto-correlation function of the green channel ($i = j = x = g$), and the cross-correlation function ($i = r$, $j = g$, $x = c$), respectively.

The $G(\tau)$ values were fit using an n-component model, with n = 2 being used for the compounds in distilled water and live cells and n = 1 being used for the D_{514} probe in culture medium:

$$G_x(\tau) = 1 + \frac{1}{N}\sum_i F_i\left(1+\frac{\tau}{\tau_i}\right)^{-1}\left(1+\frac{\tau}{s^2\tau_i}\right)^{-1/2}. \quad (2)$$

Here, F_i and τ_i are the fraction and diffusion times of component i, respectively, N is the average number of fluorescent molecules/particles in the detection volume defined by the radius w_0 and the length $2z_0$, and s is the structural parameter representing the ratio $s = z_0/w_0$. Details on the parameters and the fitting are given in refs. [34,48–50].

5. Conclusions

This study applied highly sensitive FCS and FCCS analyses to ECHO probes to examine the changes in molecular brightness, diffusion coefficients, and binding affinity with the aim of investigating the binding characteristics of the probe to the target poly(A) sequence. In addition, from an analysis of the probes as detected in live cells, it was possible to indirectly confirm the possibility that the probes were binding to the mRNA through diffusion coefficient analysis. This analysis method will be applicable to various ECHO probes for various RNA targets, and it will be of great help in quantitatively investigating the dynamic properties of intracellular RNA with high sensitivity.

Author Contributions: A.O., J.K.K. and C.-G.P. were responsible for conceptualization. A.O. and C.-G.P. were responsible for the methodology and validation. The original draft was prepared and written by B.P. and C.-G.P. The reviewing and editing were done by B.P., Y.S., Y.-M.O., C.-G.P. and J.K.K. J.K.K. and C.-G.P. were responsible for supervision. Funding acquisition was carried out by A.O., C.-G.P., J.K.K. and Y.-M.O. All authors have read and agreed to the published version of the manuscript.

Funding: This research was funded by the National Research Foundation of Korea (NRF; grant nos. 2014R1A1A2058183, 2016K2A9A2A08003729, 2018R1A5A2020732, 2019R1A2C2084122, 2020R1F1A1074033, and 2020H1D3A1A02081127), which is funded by the Korean Ministry of Science & ICT (MSIT). It was also funded by the Korea Health Industry Development Institute, funded by the Ministry of Health & Welfare, Republic of Korea (grant no. HI18C2391). This work was also supported by grant no. 2018-306, 2020IP0034-1, and 2021IP0044-1 from the Asan Institute for Life Sciences, Asan Medical Center, Seoul, Korea.

Institutional Review Board Statement: Not applicable.

Informed Consent Statement: Not applicable.

Data Availability Statement: Data is contained within the article.

Conflicts of Interest: The authors declare that they have no conflict of interest.

Abbreviations

CPS	(Fluorescence detection) counts per second
D_{nnn}	DNA-based ECHO probe of principal excitation wavelength *nnn*
DMEM	Dulbecco's modified Eagle's medium
ECHO	Exciton-controlled hybridization-sensitive oligonucleotide
FBS	Fetal bovine serum
FCS	Fluorescence correlation spectroscopy
FCCS	Fluorescence cross-correlation spectroscopy
FI	Averaged fluorescence intensity

FISH	Fluorescence in situ hybridization
GFP	Green fluorescent protein
LNA	Locked nucleic acids
mRNA	Messenger RNA
RCA	Relative cross-correlation amplitude
rRNA	Ribosomal RNA
SNP	Single nucleotide polymorphism
snRNA	Small nuclear RNA
tRNA	Transfer RNA

References

1. Armitage, B. Imaging of RNA in live cells. *Curr. Opin. Chem. Biol.* **2011**, *15*, 806–812. [CrossRef]
2. Okamoto, A. Modified ECHO probes for highly specific RNA detection in living cells. *Trends Org. Chem.* **2014**, *17*, 45–57.
3. Xia, Y.; Zhang, R.; Wang, Z.; Tian, J.; Chen, X. Recent advances in high-performance fluorescent and bioluminescent RNA imaging probes. *Chem. Soc. Rev.* **2017**, *46*, 2824–2843. [CrossRef]
4. Sollner-Webb, B.; Mougey, E.B. News from the nucleolus: rRNA gene expression. *Trends Biochem. Sci.* **1991**, *16*, 58–62. [CrossRef]
5. Matera, A.G.; Terns, R.M.; Terns, M.P. Non-coding RNAs: Lessons from the small nuclear and small nucleolar RNAs. *Nat. Rev. Mol. Cell Biol.* **2007**, *8*, 209–220. [CrossRef]
6. Schimmel, P. The emerging complexity of the tRNA world: Mammalian tRNAs beyond protein synthesis. *Nat. Rev. Mol. Cell Biol.* **2018**, *19*, 45–58. [CrossRef] [PubMed]
7. Park, H.Y.; Buxbaum, A.R.; Singer, R.H. Single mRNA Tracking in Live Cells. In *Methods in Enzymology*; Elsevier BV: Amsterdam, The Netherlands, 2010; Volume 472, pp. 387–406.
8. Bertrand, E.; Chartrand, P.; Schaefer, M.; Shenoy, S.; Singer, R.H.; Long, R.M. Localization of ASH1 mRNA Particles in Living Yeast. *Mol. Cell* **1998**, *2*, 437–445. [CrossRef]
9. Fusco, D.; Accornero, N.; Lavoie, B.; Shenoy, S.M.; Blanchard, J.-M.; Singer, R.H.; Bertrand, E. Single mRNA Molecules Demonstrate Probabilistic Movement in Living Mammalian Cells. *Curr. Biol.* **2003**, *13*, 161–167. [CrossRef]
10. Daigle, N.; Ellenberg, J. λN-GFP: An RNA reporter system for live-cell imaging. *Nat. Methods* **2007**, *4*, 633–636. [CrossRef]
11. Ozawa, T.; Natori, Y.; Sato, M.; Umezawa, Y. Imaging dynamics of endogenous mitochondrial RNA in single living cells. *Nat. Chem. Biol.* **2007**, *4*, 413–419. [CrossRef]
12. Santangelo, P.J.; Lifland, A.W.; Curt, P.; Sasaki, Y.; Bassell, G.J.; E Lindquist, M.; Crowe, J. Single molecule–sensitive probes for imaging RNA in live cells. *Nat. Methods* **2009**, *6*, 347–349. [CrossRef] [PubMed]
13. Oomoto, I.; Suzuki-Hirano, A.; Umeshima, H.; Han, Y.-W.; Yanagisawa, H.; Carlton, P.; Harada, Y.; Kengaku, M.; Okamoto, A.; Shimogori, T.; et al. ECHO-liveFISH: In vivo RNA labeling reveals dynamic regulation of nuclear RNA foci in living tissues. *Nucleic Acids Res.* **2015**, *30*, e126. [CrossRef] [PubMed]
14. Ainger, K.; Avossa, D.; Morgan, F.; Hill, S.J.; Barry, C.; Barbarese, E.; Carson, J.H. Transport and localization of exogenous myelin basic protein mRNA microinjected into oligodendrocytes. *J. Cell Biol.* **1993**, *123*, 431–441. [CrossRef] [PubMed]
15. Ishihama, Y.; Funatsu, T. Single molecule tracking of quantum dot-labeled mRNAs in a cell nucleus. *Biochem. Biophys. Res. Commun.* **2009**, *381*, 33–38. [CrossRef] [PubMed]
16. Smith, A.M.; Duan, H.; Mohs, A.; Nie, S. Bioconjugated quantum dots for in vivo molecular and cellular imaging. *Adv. Drug Deliv. Rev.* **2008**, *60*, 1226–1240. [CrossRef]
17. Knowles, R.B.; Sabry, J.H.; Martone, M.E.; Deerinck, T.J.; Ellisman, M.H.; Bassell, G.J.; Kosik, K.S. Translocation of RNA Granules in Living Neurons. *J. Neurosci.* **1996**, *16*, 7812–7820. [CrossRef] [PubMed]
18. De Brabander, M.; Geuens, G.; Nuydens, R.; Moeremans, M.; De Mey, J. Probing microtubule-dependent intracellular motility with nanometre particle video ultramicroscopy (nanovid ultramicroscopy). *Cytobios* **1985**, *43*, 273–283.
19. Pack, C.-G.; Paulson, B.; Shin, Y.; Jung, M.K.; Kim, J.S. Variably Sized and Multi-Colored Silica-Nanoparticles Characterized by Fluorescence Correlation Methods for Cellular Dynamics. *Materials* **2020**, *14*, 19. [CrossRef]
20. Silverman, A.P.; Kool, E.T. Quenched probes for highly specific detection of cellular RNAs. *Trends Biotechnol.* **2005**, *23*, 225–230. [CrossRef]
21. Samanta, D.; Ebrahimi, S.B.; Mirkin, C.A. Nucleic-Acid Structures as Intracellular Probes for Live Cells. *Adv. Mater.* **2020**, *32*, e1901743. [CrossRef]
22. Ikeda, S.; Kubota, T.; Yuki, M.; Okamoto, A. Exciton-Controlled Hybridization-Sensitive Fluorescent Probes: Multicolor Detection of Nucleic Acids. *Angew. Chem. Int. Ed.* **2009**, *17*, 6480–6484. [CrossRef]
23. Sugizaki, K.; Okamoto, A. ECHO-LNA Conjugates: Hybridization-Sensitive Fluorescence and Its Application to Fluorescent Detection of Various RNA Strands. *Bioconjug. Chem.* **2010**, *21*, 2276–2281. [CrossRef] [PubMed]
24. Kubota, T.; Ikeda, S.; Yanagisawa, H.; Yuki, M.; Okamoto, A. Cy5-Conjugated Hybridization-Sensitive Fluorescent Oligonucleotides for Ratiometric Analysis of Nuclear Poly(A)+ RNA. *Bioconjug Chem.* **2011**, *22*, 1625–1630. [CrossRef]
25. Sato, S.; Watanabe, M.; Katsuda, Y.; Murata, A.; Wang, D.O.; Uesugi, M. Live-Cell Imaging of Endogenous mRNAs with a Small Molecule. *Angew. Chem. Int. Ed.* **2015**, *54*, 1855–1858. [CrossRef] [PubMed]

26. Slomovic, S.; Fremder, E.; Staals, R.H.G.; Pruijn, G.J.M.; Schuster, G. Addition of poly(A) and poly(A)-rich tails during RNA degra-dation in the cytoplasm of human cells. *Proc. Natl. Acad. Sci. USA* **2010**, *107*, 7407–7412. [CrossRef]
27. Trcek, T.; Larson, D.R.; Moldón, A.; Query, C.C.; Singer, R.H. Single-Molecule mRNA Decay Measurements Reveal Promoter-Reg-ulated mRNA Stability in Yeast. *Cell* **2011**, *147*, 1484–1497. [CrossRef] [PubMed]
28. Liang, L.; Wang, X.; Xing, D.; Chen, T.; Chen, W.R. Noninvasive determination of cell nucleoplasmic viscosity by fluorescence correlation spectroscopy. *J. Biomed. Opt.* **2009**, *14*, 024013. [CrossRef]
29. Szczepański, K.; Kwapiszewska, K.; Holyst, R. Stability of cytoplasmic nanoviscosity during cell cycle of HeLa cells synchronized with Aphidicolin. *Sci. Rep.* **2019**, *9*, 1–8. [CrossRef] [PubMed]
30. Bacia, K.; A Kim, S.; Schwille, P. Fluorescence cross-correlation spectroscopy in living cells. *Nat. Methods* **2006**, *3*, 83–89. [CrossRef]
31. Wobma, H.M.; Blades, M.L.; Grekova, E.; McGuire, D.L.; Chen, K.; Chan, W.C.W.; Cramb, D.T. The development of direct multicolour fluo-rescence cross-correlation spectroscopy: Towards a new tool for tracking complex biomolecular events in real-time. *Phys. Chem. Chem. Phys.* **2012**, *14*, 3290. [CrossRef]
32. Santra, S.; Bagwe, R.P.; Dutta, D.; Stanley, J.T.; Walter, G.A.; Tan, W.; Moudgil, B.M.; Mericle, R.A. Synthesis and Characterization of Fluorescent, Radio-Opaque, and Paramagnetic Silica Nanoparticles for Multimodal Bioimaging Applications. *Adv. Mater.* **2005**, *17*, 2165–2169. [CrossRef]
33. Lee, W.; Lee, Y.-I.; Lee, J.; Davis, L.M.; Deininger, P.; Soper, S.A. Cross-Talk-Free Dual-Color Fluorescence Cross-Correlation Spec-troscopy for the Study of Enzyme Activity. *Anal. Chem.* **2010**, *82*, 1401–1410. [CrossRef]
34. Pack, C.G.; Song, M.R.; Tae, E.L.; Hiroshima, M.; Byun, K.H.; Kim, J.S.; Sako, Y. Microenvironments and different nanoparticle dynamics in living cells revealed by a standard nanoparticle. *J. Control. Release* **2012**, *163*, 315–321. [CrossRef]
35. Shin, H.-S.; Okamoto, A.; Sako, Y.; Kim, S.W.; Kim, S.Y.; Pack, C.-G. Characterization of the Triplet State of Hybridization-Sensitive DNA Probe by Using Fluorescence Correlation Spectroscopy. *J. Phys. Chem. A* **2013**, *117*, 27–33. [CrossRef] [PubMed]
36. Ikeda, S.; Okamoto, A. Hybridization-Sensitive On–Off DNA Probe: Application of the Exciton Coupling Effect to Effective Fluorescence Quenching. *Chem. Asian J.* **2008**, *3*, 958–968. [CrossRef]
37. Shin, H.-S.; Okamoto, A.; Sako, Y.; Kim, S.W.; Kim, S.Y.; Pack, C.-G. Radiationless deactivation of hybridization-sensitive DNA probe. *J. Lumin.* **2012**, *132*, 2566–2571. [CrossRef]
38. Elkon, R.; Ugalde, A.P.; Agami, R. Alternative cleavage and polyadenylation: Extent, regulation and function. *Nat. Rev. Genet.* **2013**, *14*, 496–506. [CrossRef] [PubMed]
39. Lukacs, G.L.; Haggie, P.; Seksek, O.; Lechardeur, D.; Freedman, N.; Verkman, A.S. Size-dependent DNA Mobility in Cytoplasm and Nucleus. *J. Biol. Chem.* **2000**, *275*, 1625–1629. [CrossRef]
40. Takagi, T.; Kii, H.; Kinjo, M. DNA Measurements by Using Fluorescence Correlation Spectroscopy and Two-Color Fluorescence Cross Correlation Spectroscopy. *Curr. Pharm. Biotechnol.* **2004**, *5*, 199–204. [CrossRef] [PubMed]
41. Kubota, T.; Ikeda, S.; Yanagisawa, H.; Yuki, M.; Okamoto, A. Hybridization-Sensitive Fluorescent Probe for Long-Term Monitoring of Intracellular RNA. *Bioconjug. Chem.* **2009**, *20*, 1256–1261. [CrossRef]
42. Pack, C.; Saito, K.; Tamura, M.; Kinjo, M. Microenvironment and Effect of Energy Depletion in the Nucleus Analyzed by Mobility of Multiple Oligomeric EGFPs. *Biophys. J.* **2006**, *91*, 3921–3936. [CrossRef]
43. Tyagi, S.; Bratu, D.P.; Kramer, F.R. Multicolor molecular beacons for allele discrimination. *Nat. Biotechnol.* **1998**, *16*, 49–53. [CrossRef] [PubMed]
44. Kuhn, H.; Demidov, V.V.; Coull, J.M.; Fiandaca, M.J.; Gildea, B.D.; Frank-Kamenetskii, M.D. Hybridization of DNA and PNA Molecular Beacons to Single-Stranded and Double-Stranded DNA Targets. *J. Am. Chem. Soc.* **2002**, *124*, 1097–1103. [CrossRef]
45. Bratu, D.P.; Cha, B.-J.; Mhlanga, M.M.; Kramer, F.R.; Tyagi, S. Visualizing the distribution and transport of mRNAs in living cells. *Proc. Natl. Acad. Sci. USA* **2003**, *100*, 13308–13313. [CrossRef] [PubMed]
46. Tadakuma, H.; Ishihama, Y.; Shibuya, T.; Tani, T.; Funatsu, T. Imaging of single mRNA molecules moving within a living cell nucleus. *Biochem. Biophys. Res. Commun.* **2006**, *344*, 772–779. [CrossRef] [PubMed]
47. Hayashi, G.; Yanase, M.; Takeda, K.; Sakakibara, D.; Sakamoto, R.; Wang, D.O.; Okamoto, A. Hybridization-Sensitive Fluorescent Oligonu-cleotide Probe Conjugated with a Bulky Module for Compartment-Specific mRNA Monitoring in a Living Cell. *Bioconjug. Chem.* **2015**, *26*, 412–417. [CrossRef]
48. Ow, H.; Larson, D.R.; Srivastava, M.; Baird, B.A.; Webb, W.W.; Wiesner, U. Bright and Stable Core−Shell Fluorescent Silica Nano-particles. *Nano Lett.* **2005**, *5*, 113–117. [CrossRef] [PubMed]
49. Martinez-Moro, M.; Di Silvio, D.; Moya, S.E. Fluorescence correlation spectroscopy as a tool for the study of the intracellular dynamics and biological fate of protein corona. *Biophys. Chem.* **2019**, *253*, 106218. [CrossRef]
50. Pack, C.-G.; Yukii, H.; Toh-E, A.; Kudo, T.; Tsuchiya, H.; Kaiho, A.; Sakata, E.; Murata, S.; Yokosawa, H.; Sako, Y.; et al. Quantitative live-cell imaging reveals spatio-temporal dynamics and cytoplasmic assembly of the 26S proteasome. *Nat. Commun.* **2014**, *5*, 3396. [CrossRef] [PubMed]